

AVO NMO

Jonathan E. Downton and Laurence R. Lines – University of Calgary

CSEG Geophysics 2002

SUMMARY

This paper demonstrates a methodology to perform AVO and NMO inversion simultaneously using suitable constraints from the external well control or empirical rock physical relationships. Using synthetic data, it is shown this new methodology generates superior reflectivity estimates compared to the traditional approach of performing NMO followed by AVO inversion.

INTRODUCTION

The input to AVO inversion, such as Fatti et al. (1994), Shuey (1985) and Smith and Gidlow (1987), for most land seismic data are seismic gathers after NMO. NMO is a kinematic correction that distorts the amplitudes in an offset dependent fashion. This distortion subsequently negatively impacts the AVO inversion estimates. The problem becomes more pronounced as the maximum angle used for the AVO inversion is increased. In contrast to this, the uncertainty of AVO reflectivity attribute estimates due to random noise decrease as the range of angles used for the inversion increase (Downton and Lines, 2001a). This suggests some sort of trade off between the two concerns. There would be an advantage if we could minimize the error introduced by the NMO so larger angles could be used. Further, there is a desire in the industry to do 3 term AVO inversions, inverting for density. For accurate results, this requires gathers with large incidence angles.

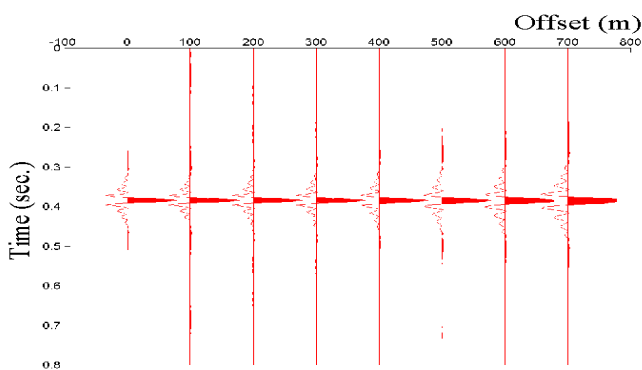


Figure 1: Synthetic gather for a single spike after NMO for incident angles from 0 to 45 degrees. Note how NMO stretch lowers the frequency on the far offsets and changes the wavelet character.

NMO stretch (Dunkin and Levin, 1973) is an example of an amplitude distortion introduced by the NMO process. Figure 1 shows a gather after NMO for incident angles from 0 to 45

degrees. The model generating this is a single reflector or spike convolved with a 5/10-60/70 Hz band pass filter. Ideally after NMO, this reflector should have a constant waveform and amplitude. It does not. The far offsets are noticeably lower frequency than the near offsets and the overall character changes as a function of offset.

AVO is typically performed on a sample-by-sample basis. If the waveform changes as a function of offset this will distort the results of the AVO analysis particularly for samples that are not directly on the peak or trough of the wavelet. If for example, one was inverting for the normal incident P-impedance reflectivity and the gradient (Shuey, 1985), the offset dependent waveform changes introduced by the NMO will bias the gradient (Swan, 1997). Likewise, the estimates of other AVO reflectivity attributes such as the P- and S-impedance reflectivity (Fatti et al., 1994) will be biased. Both cases will result in scatter in the cross-plot space. This will blur anomalies and potentially obscure small anomalies into the background trend.

NMO can be written as a matrix operator (Claerbout, 1992) and theoretically its inverse can be found. If this is done, NMO would not introduce amplitude distortions. However, in practice this is not usually done since the problem is underdetermined and ill conditioned. Conceptually, this can be understood by noting that the reflectivity of the "far offset trace", is time delayed and squeezed into a smaller time window relative to that of the "zero offset trace". If both the zero offset and the far offset reflectivity data are high cut filtered, the far offset data will contain less information after filtering than the near offset data. In the time domain this effect manifests itself as offset dependent tuning (Lin and Phair, 1993). The high cut filter introduces a null space into the NMO matrix operator.

In light of these issues, various papers have suggested methodologies on how to prepare the seismic data prior to AVO. Ursin and Ekren (1995) suggested flattening the CDP gather on a particular event rather than performing NMO. This avoids NMO stretch, but does not deal with the offset dependent tuning. In this paper, we will demonstrate an approach where the AVO and NMO inversion problems are treated simultaneously. The problem is ill-posed, but constraints similar to Downton and Lines (2001b) can be incorporated through a Bayesian framework to stabilize the problem. In the first section of this paper, the theory of this simultaneous AVO NMO inversion will be developed. In the second half, the method will be shown to give superior results on synthetic data compared to the traditional approach.

THEORY

Convolutional model

The convolutional model is used as the basis for this AVO NMO inversion scheme. This model assumes the earth is composed of a series of flat homogenous isotropic layers. The Zoeppritz equations or some approximation of them are used to model how the reflectivity changes as a function of offset. Ray tracing is done to map the relationship between the angle of incidence and offset. Transmission losses, converted waves and multiples are not incorporated in this model and so must be addressed through prior processing. In theory, gain corrections such as spherical divergence, absorption, directivity and array corrections can be incorporated into this model, but are not considered in this abstract for brevity and simplicity.

The 2 term Fatti approximation (Fatti et al. 1994, equation 4) will be used to approximate the Zoeppritz equation

$$x(\theta) = [1 + \tan^2 \theta] R_{IP} - \left[8 \left(\frac{V_s}{V_p} \right)^2 \sin^2 \theta \right] R_{IS}, \quad (1)$$

where θ is the average angle of incidence, $x(\theta)$ is the offset dependent reflectivity, V_p and V_s are the P- and S-wave velocity, R_{IP} and R_{IS} are the P- and S-impedance reflectivity respectively. Equation (1) can be written in matrix form. For example consider the case when there is two offsets, a near offset $d^{(1)}$ and a far offset $d^{(2)}$ then

$$\begin{bmatrix} x^{(1)} \\ x^{(2)} \end{bmatrix} = \begin{bmatrix} f^{(1)} & g^{(1)} \\ f^{(2)} & g^{(2)} \end{bmatrix} \begin{bmatrix} R_{IP} \\ R_{IS} \end{bmatrix}, \quad (2)$$

where $f^{(n)} = [1 + \tan^2 \theta^{(n)}]$, and $g^{(n)} = 8 \frac{V_s^2}{V_p^2} \sin^2 \theta^{(n)}$ and the superscript indicates the offset.

Typically equation (2) is solved for on an interface by interface basis, where each interface corresponds to a time sample. This ignores the band limited nature of the seismic data. To address this, equation (2) can be modified to solve for multiple time samples simultaneously. To illustrate this, consider the case with 2 interfaces, equation (2) becomes

$$\begin{bmatrix} x_1^{(1)} \\ x_1^{(2)} \\ x_2^{(1)} \\ x_2^{(2)} \end{bmatrix} = \begin{bmatrix} f_1^{(1)} & g_1^{(1)} & 0 & 0 \\ f_1^{(2)} & g_1^{(2)} & 0 & 0 \\ 0 & 0 & f_2^{(1)} & g_2^{(1)} \\ 0 & 0 & f_2^{(2)} & g_2^{(2)} \end{bmatrix} \begin{bmatrix} R_{IP1} \\ R_{IS1} \\ R_{IP2} \\ R_{IS2} \end{bmatrix}, \quad (3)$$

where the subscript has been introduced to notate the interface number. This can be rearranged so that it is ordered along common offsets rather than common time samples

$$\begin{bmatrix} x_1^{(1)} \\ x_2^{(1)} \\ x_1^{(2)} \\ x_2^{(2)} \end{bmatrix} = \begin{bmatrix} f_1^{(1)} & 0 & g_1^{(1)} & 0 \\ 0 & f_2^{(1)} & 0 & g_2^{(1)} \\ f_1^{(2)} & 0 & g_1^{(2)} & 0 \\ 0 & f_2^{(2)} & 0 & g_2^{(2)} \end{bmatrix} \begin{bmatrix} R_{IP1} \\ R_{IP2} \\ R_{IS1} \\ R_{IS2} \end{bmatrix}. \quad (4)$$

This can be further simplified by writing the elements composing a common offset as vectors

$$\begin{bmatrix} \mathbf{x}_1 \\ \mathbf{x}_2 \end{bmatrix} = \begin{bmatrix} \mathbf{F}_1 & \mathbf{G}_1 \\ \mathbf{F}_2 & \mathbf{G}_2 \end{bmatrix} \begin{bmatrix} \mathbf{r}_{IP} \\ \mathbf{r}_{IS} \end{bmatrix}, \quad (5)$$

where the elements of linear operator matrix are diagonal matrices composed of their respective weights for each offset.

AVO NMO

NMO can be written as a linear operator (Claerbout 1992). A reflectivity sequence referenced to zero offset time \mathbf{x}_n can be transformed to offset dependent travel time \mathbf{d}_n by the linear operator \mathbf{N}_n so that

$$\mathbf{d}_n = \mathbf{N}_n \mathbf{x}_n. \quad (6)$$

The matrix \mathbf{N}_n can be constructed using whatever offset/ travel time relationship one desires. In order to invert data at large angles of incidences it is important to correctly position the event without introducing residual NMO. In this case, we use a higher order correction following Castle (1994).

Constrained Inversion

Combining equations (5) and (6) results in the set of linear equations that may be used to solve NMO and AVO simultaneously.

$$\begin{bmatrix} \mathbf{d}_1 \\ \mathbf{d}_2 \end{bmatrix} = \begin{bmatrix} \mathbf{N}_1 \mathbf{F}_1 & \mathbf{N}_1 \mathbf{G}_1 \\ \mathbf{N}_2 \mathbf{F}_2 & \mathbf{N}_2 \mathbf{G}_2 \end{bmatrix} \begin{bmatrix} \mathbf{r}_{IP} \\ \mathbf{r}_{IS} \end{bmatrix}. \quad (7)$$

Equation (7) may be generalized for more offsets and interfaces. Note that \mathbf{N} , \mathbf{F} and \mathbf{G} are sparse matrices and can be quickly calculated. Equation (7) may be further modified to include the mute and gain corrections.

The AVO problem is typically overdetermined, while the NMO problem is underdetermined for the reasons outlined in the introduction. This means that linear operator in equation (7) is mixed-determined and its inverse will be ill-conditioned. Constraints can be introduced using a Bayesian framework similar to Downton and Lines (2001b) to make the problem better conditioned.

EXAMPLE

A simple geologic model (Figure 2) was constructed to test this approach. The background P-wave velocity is simply a linear function of depth. Three anomalies were introduced onto this background trend, each generating a positive reflection at top and a negative reflection at the base. The top and basal

reflections will tune in an offset dependent fashion as discussed in the introduction. The S-velocity follows the mudrock trend (Castagna et al. 1985) with the exception of the last anomaly where the Vp/Vs ratio has been set to simulate a gas anomaly. The density follows the background P-wave velocity trend using the Gardner relationship (Gardner et al. 1974) thus the density reflectivity will be zero over the range of frequencies used in the modeling. This was done so we could ignore any potential error being introduced by the fact we are using a two-term rather than three term AVO inversion, thus simplifying our analysis of the results.

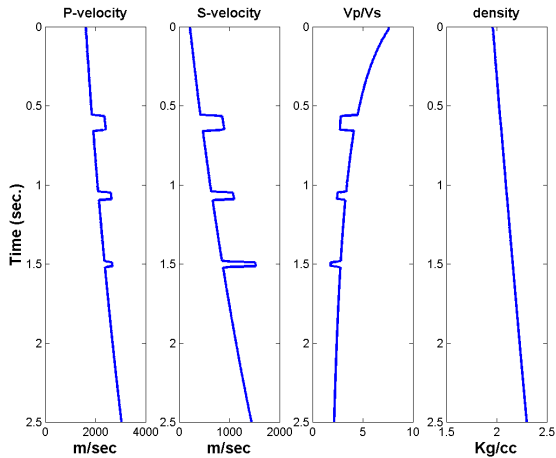


Figure 2: Velocity and density input to synthetic model.

A synthetic gather was generated based on the model shown in Figure 2, using the Zoeppritz equation and ray tracing. The resulting gather was filtered with a 5/10-60/70 Hz band pass filter and muted for angles beyond 45 degrees (left panel Figure 3). This gather was then NMO corrected (middle panel Figure 3). The NMO correction was done with sinc interpolation. Also shown in the right panel of Figure 3, for reference, is a synthetic gather generated without NMO. The synthetic gather with NMO has much lower frequency on the far offsets than the synthetic gather generated without NMO. Further, one can observe offset dependent tuning on the synthetic gather particularly on the last reflector.

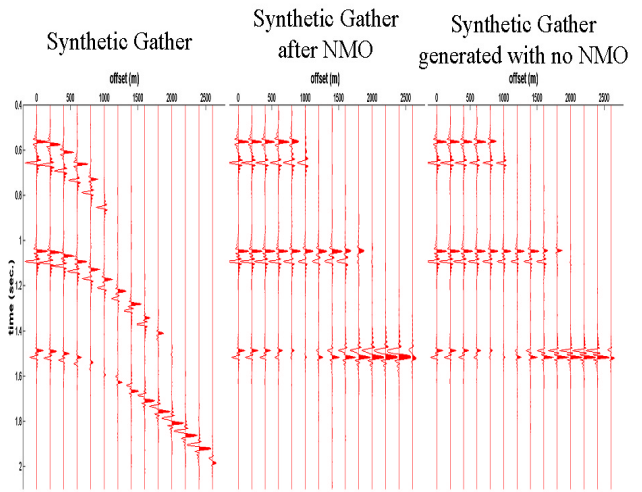


Figure 3: (left panel) Synthetic gather generated by Zoeppritz equation and ray tracing followed by NMO, (middle panel) synthetic gather after NMO, (right panel) synthetic gather generated without NMO.

This gather was inverted two ways, once using the traditional methodology of applying NMO and then performing the AVO inversion (Figure 4) and once using the new methodology of doing the simultaneous AVO NMO inversion (Figure 5). Both methodologies used the same RMS velocity and shifting parameter and angles up to 45 degrees for the AVO inversion. The results shown in Figure 4 and 5 are shown with a 5/10-50/60 Hz filter. If the results were shown with a 5/10-60/70 Hz filter there would be high frequency ringing on the S-impedance reflectivity.

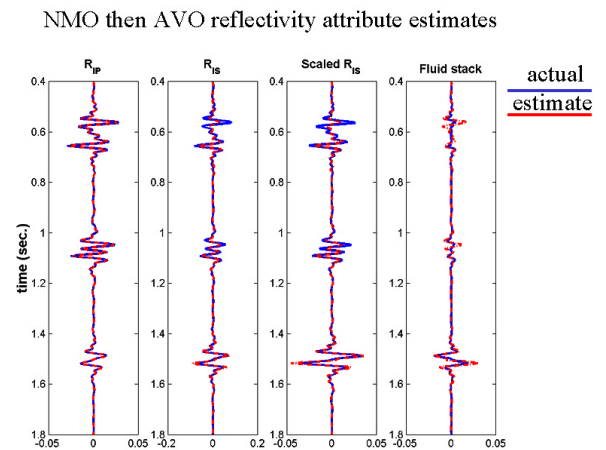


Figure 4: AVO inversion results after performing NMO and then doing AVO inversion. Note that the estimate of the S-impedance reflectivity is poor for the reflector at 0.6 seconds resulting in the poor fluid stack estimate.

AVO NMO reflectivity attribute estimates

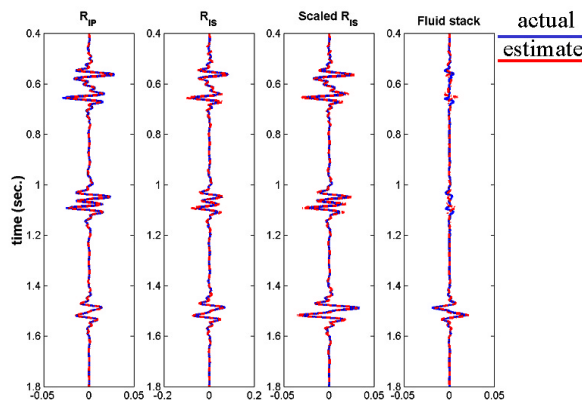


Figure 5: AVO inversion results of doing the simultaneous NMO AVO inversion. Note that the estimate of the fluid stack for all reflections is much better than the traditional methodology (Figure 4)

For both flows a fluid stack (Smith and Gidlow, 1987) was generated. In the case where the S-velocity follows the P-wave velocity there should be no reflection. This should be the case for the top two anomalies at 0.6 and 1.05 seconds. In the case of a gas sand there should be an anomalous trough followed by a peak. This should be the case for the anomaly at 1.5 seconds.

The estimate of the fluid stack following the traditional approach (figure 5) shows fluid stack anomalies at all three levels. This is a result of the S-impedance reflectivity being underestimated by the inversion due to artifacts introduced by the NMO. The fluid stack generated by the simultaneous AVO NMO inversion shows a much better match between the estimate and the reference.

CONCLUSIONS

In this synthetic example the simultaneous AVO NMO inversion gave better results than traditional approach of first applying NMO and then doing the AVO inversion. This is consistent with expectations, since the way NMO is traditionally applied will introduce amplitude and character distortions. The improvement is even true for an event showing significant offset dependent tuning such as the reflector at 1.5 seconds. In general the estimate of P and S-impedance reflectivity track each other better on a sample-by-sample basis. This leads to less scatter and distortion being introduced in the cross-plot space.

These improvements come at a significant computational cost. Instead of solving N inverse problems each with 2 parameters, the simultaneous AVO NMO inversion solves for $2*N$ parameters, where N is the number of time samples. These costs can be abated somewhat since the problem is sparse and efficient large scale optimization algorithms can be used to solve the problem.

Even after applying the simultaneous AVO NMO inversion methodology we were unable to accurately recover the same frequency range as input into the inversion for the S-impedance reflectivity. Our estimate was about 10 Hz lower frequency than the input. This is most likely due to loss of frequency information as function of offset discussed in the introduction.

ACKNOWLEDGEMENTS

The authors would like to thank Scott Pickford, N.S.E.R.C. and the C.R.E.W.E.S. sponsors for funding this research. In addition, the authors thank Yongyi Li of Scott Pickford for his helpful suggestions.

REFERENCES

- Castagna, J. P., Batzle, M.L., and Eastwood, R.L., 1985, Relationships between compressional-wave and shear-wave velocities in clastic silicate rocks: *Geophysics*, **50**, 571-581.
- Castle, R.J., 1994, Theory of normal moveout: *Geophysics*, **59**, 983-999.
- Claerbout J.F., 1992, *Earth Soundings Analysis, Processing versus Inversion*, Blackwell Scientific Publications, 110-120.
- Downton, J. and Lines, L., 2001a, AVO feasibility and reliability analysis, *CSEG recorder*, Vol. 26, No 6, 66-73.
- Downton, J. and Lines, L., 2001b, Constrained 3 parameter AVO estimation and uncertainty analysis, 71st Ann. Mtg., Soc. Expl. Geophys., Expanded Abstracts, 251-254.
- Dunkin, J.W., and Levin, F.K., 1973, Effect of normal moveout on a seismic pulse: *Geophysics*, **38**, 635-642.
- Fatti, J.L., Smith, G.C., Vail, P.J., Strauss, P.J., and Levitt, P.R., 1994, Detection of gas in sandstone reservoirs using AVO analysis: A 3-D seismic case history using the Geostack technique: *Geophysics*, **59**, 1362-1376.
- Gardner, G.H.F., Gardner, L.W. and Gregory, A.R., 1974, Formation velocity and density - The diagnostic basics for stratigraphic traps: *Geophysics*, **39**, 770-780.
- Shuey, R.T., 1985, A simplification of the Zoeppritz equations: *Geophysics*, **50**, 609-614.
- Smith, G.C., and Gidlow, P.M., 1987, Weighted stacking for rock property estimation and detection of gas: *Geophys. Prosp.*, **35**, 993-1014.
- Swan, H.W., 1997, Removal of offset-dependent tuning in AVO analysis, 67th Ann. Internat. Mtg: Soc. of Expl. Geophys., 175-178.
- Ursin, B. and Ekren, B.O., 1995, Robust AVO analysis: *Geophysics*, **60**, 317-326.